GEOCHIMICA BRASILIENSIS 16(1): 079-097, 2002

SULFUR STABLE ISOTOPE SIGNATURES OF THE MORRO DA PEDRA PRETA FORMATION, SERRA DO ITABERABA GROUP, SÃO PAULO STATE, BRAZIL

G.M. Garda[1], P. Beljavskis[1], C. Juliani[1], A.J. Boyce[2]

1. Instituto de Geociências da Universidade de São Paulo, Rua do Lago, 562, CEP 05508-080, São Paulo, SP, Brazil
2. Scottish Universities Environmental Research Centre, Rankine Avenue, East Kilbride, Glasgow G75 0QF, Scotland

Recebido em 03/02; aprovado para publicação em 09/02

ABSTRACT

The Serra do Itaberaba Group (São Paulo - Brazil) was explored in the XVIII century for gold. Sulfur stable isotope data helped constrain four sulfidation stages that affected the basal, Morro da Pedra Preta Formation metavolcanic-sedimentary sequence. Syn-sedimentary pyrrhotite from Stage I (–5.47 per mil < $\delta^{34}S$ < –8.7 per mil) and Stage II (+4.48 per mil < $\delta^{34}S$ < +7.36 per mil) sulfides resulted respectively from bacterial and thermochemical reduction of seawater sulfate. The $\delta^{34}S$ values obtained for both stages also reveal an igneous sulfur component, derived either from the volcanic pile being leached by hydrothermal fluids, or intruding andesite and dacite bodies that powered seawater circulation through the sequence.

Free gold is associated with chalcocite and covellite after Stage III chalcopyrite (+3.6 per mil < $\delta^{34}S$ < +2.6 per mil). Pyrite predominates in Stage IV (+2.4 per mil < $\delta^{34}S$ < +2.9 per mil). Lower-temperature, submicroscopic galena ($\delta^{34}S$ ª +1 per mil), Ag-bearing Bi tellurides and REE minerals fill cavities and fractures in sulfides of previous stages. Molybdenite ($\delta^{34}S$ ª +3 per mil) and scheelite are associated with stages III and IV and related to late fluids derived from nearby Neoproterozoic granite bodies. The influence of meteoric water is not ruled out at stages III and IV, once post-magmatic fluids circulated along fault and fracture systems that crosscut the Morro da Pedra Preta Formation.

RESUMO

No século XVIII foi explorado ouro do Grupo Serra do Itaberaba (São Paulo - Brasil). Quatro estágios de sulfetização que afetaram a seqüência basal metavulcano-sedimentar Formação Morro da Pedra Preta são caracterizados por isótopos estáveis de enxofre. Pirrotita sin-sedimentar do Estágio I (–5.47 per mil < $\delta^{34}S$ < –8.7 per mil) e sulfetos do Estágio II (+4.48 per mil < $\delta^{34}S$ < +7.36 per mil) resultaram respectivamente da redução bacteriana e da redução termoquímica de sulfato da água do mar. Os valores de $\delta^{34}S$ obtidos para ambos os estágios também revelam um componente ígneo, derivado ou da pilha vulcânica lixiviada por fluidos hidrotermais, ou de corpos de andesito e dacito, cujo calor promoveu a circulação da água do mar pela seqüência.

Ouro livre associa-se com calcosina e covelita, formadas a partir de calcopirita do Estágio III (+3.6 per mil < $\delta^{34}S$ < +2.6 per mil). Pirita predomina no Estágio IV (+2.4 per mil < $\delta^{34}S$ < +2.9 per mil). Galena ($\delta^{34}S$ ª +1 per mil), teluretos de Bi contendo Ag e minerais de ETR preenchem cavidades e fraturas em sulfetos dos estágios anteriores. Molibdenita ($\delta^{34}S$ ª +3 per mil) e scheelita associam-se aos estágios III e IV e a fluidos tardios derivados de corpos graníticos neoproterozóicos vizinhos. Água meteórica pode ter interferido nos estágios III e IV, uma vez que os fluidos pós-magmáticos circularam por sistemas de falhas e fraturas que cortam a Formação Morro da Pedra Preta.

INTRODUCTION

In São Paulo State (Brazil), gold occurs in Precambrian metamorphosed sequences, namely the Açungui, Serra do Itaberaba and São Roque groups and Embu and Varginha complexes. The Serra do Itaberaba Group (Guarulhos, São Paulo) was the scenario of gold exploration and mining in the XVI and XVII centuries. Alluvial deposits along the Ribeirão das Lavras (Noronha, 1960) were exploited, employing natives as slaves (Juliani *et al.*, 1995). São Paulo was no longer the pole of gold exploration after the exhaustion of the mines and the finding of richer gold deposits in Minas Gerais, Bahia, Goiás and Mato Grosso by the *bandeirantes*. At present, Guarulhos and its neighbouring industrial areas are highly populated.

In the early 80's, the Technological Research Institute of São Paulo State (IPT) developed several projects aiming at the evaluation of gold-bearing terrains (IPT, 1981; IPT, 1982; IPT, 1984; IPT, 1985; IPT, 1986; IPT, 1987; IPT, 1988;IPT, 1993). In the surroundings of Guarulhos, Au concentrations between 0.1-1.5 g/m^3 were detected in the 0.5-2.5 m-thick colluvium of the Ribeirão das Lavras (Juliani *et al.*, 1995), as well as in the 1.0 to 1.4 m-thick alluvium, containing 0.2 to 0.36 g Au/m^3. A sample from a gravel level within this alluvial deposit contained nuggets with up to 0.42 g. Panning concentrates revealed fine-grained gold (< 0.15 mm) and rare nuggets with more than 1 mm in diameter.

Since the 90's, detailed laboratory studies have been carried out in order to better characterize types of gold mineralization in The Serra do Itaberaba Group, in particular in the areas informally named Tapera Grande and Quartzito.

Based on available data, reflected light microscopy and preliminary scanning electron microscopy imagery and mineral analyses (SEM-EDS), Beljavskis *et al.* (1993) proposed a syngenetic and an epigenetic origin for gold for the Tapera Grande area. This proposal has been improved lately with the acquisition of more detailed SEM-EDS and stable isotope data. This paper will focus on S stable isotope analyses, which helped reevaluate the model suggested for the mineralizations in the Morro da Pedra Preta Formation.

THE SERRA DO ITABERABA GROUP

The Serra do Itaberaba and São Roque groups are two distinct supracrustal rock sequences located north of the Taxaquara and Rio Jaguari shear zones (Fig. 1a).

The São Roque Group is essentially a metasedimentary unit composed of metarkoses with metabasite lenses at the base, overlain by metaconglomerates, feldspatic quartzites and metarhythmites with subordinate lenses of carbonatic rocks. These sediments, deposited in alluvial fan and coastal environments, were covered by a transgressive marine sequence. Volcanic and volcaniclastic activity is rare. The São Roque Group was deposited in the Neoproterozoic (Hackspacker *et al.*, 1999) and lies unconformably on the Serra do Itaberaba Group, the contacts being in part erosional but more conspicuously along thrust zones.

The Morro da Pedra Preta Formation metavolcanic-sedimentary sequence is the basal unit of the Serra do Itaberaba Group, overlain by andaluzite-rich metapelites and iron-manganiferous schists of the Nhanguçu Formation, and by quartz schists of the Pirucaia Formation (Juliani, 1993; Juliani & Beljavskis, 1995). The volcanic rocks are predominantly of basic composition and were deposited in a MOR environment. Southwestwards, coarser-grained clastic sediments predominate (Fig. 1a), the volcanic and volcaniclastic contribution being much more reduced, indicating depositional environments proximal to the continental margin (Juliani, 2000).

The deposition age is still uncertain, but metaspilites from pillow lavas of the Morro da Pedra Preta Formation yielded K-Ar ages of 1692 ± 157 Ma (Juliani *et al.*, 1986), and a zircon U-Pb dating for metandesites intrusive in metabasalts and associated tuffs resulted in 1395 ± 10 Ma (Juliani *et al.*, 2000). This age is interpreted as the maximum age for the clastic sedimentation in the Morro da Pedra Preta Formation and marks the beginning of the oceanic basin subsidence, once the metandesites were generated by the subduction of a distal ensimatic plate (Juliani, 1993). Metarhyolite bodies hosted by the Nhanguçu Formation present two zircon populations, an older one of 1449 ± 3 Ma and a younger one of 619 ± 3 Ma, being the former interpreted as zircons inherited from the Morro da Pedra Preta Formation volcanic sequence and the latter, as zircons from the acid magmatism coeval with the São Roque Group (Juliani *et al.*, 2000).

The São Roque Group underwent low-pressure metamorphic regime that barely reached the medium grade, suggesting an

intracrustal or back-arc evolution. The Serra do Itaberaba Group was polymetamorphosed, being affected by an older medium-pressure event with a baric peak around 7.5 kbar, reaching the upper amphibolite facies (~ 640° C) northwestwards, grading to the transitional greenschist facies southwestwards (Juliani *et al.*, 2000). The second event was at most a medium-grade metamorphism, less strong than the previous event, and it took place under low-pressure conditions, which indicates a correlation with the metamorphic event that affected the São Roque Group.

The Morro da Pedra Preta Formation was deposited in an oceanic basin environment. The **metabasites** form complexly deformed, elongated bodies, generally made of several pilled flows. They are essentially represented by amphibolites and hornblende schists, with subordinate metadiabases, metagabbros and small bodies of metandesites and metadacites. **Volcanic** and **volcaniclastic** rocks are represented by basic and intermediate tuffs, hyaloclastite and autoclastic tuffs or breccias, with fragments of basalt and andesite. Garnet and magnetite are common metamorphic accessory minerals and can locally reach higher concentrations, varying between 5% and 10%. They are predominantly fine to medium-grained hornblende schist and biotite-hornblende schist. Such rocks occur in close association with metavolcaniclastic rocks. Grading and interbedding with metavolcaniclastic and calc-silicate rocks and tuffaceous metasediments are common (Juliani & Beljavskis, 1983).

Metapelites are represented by banded schists, classified by their quartz, biotite, muscovite, cordierite, garnet, staurolite, kyanite, andaluzite and sillimanite contents. **Graphitic metapelites**, in general with high sulfide contents, deposited on the volcanic/volcaniclastic sequence, contain variable percentages of graphite and constitute small bodies with maximum thickness of a few dozen meters and sometimes extending for more than a hundred meters. Reducing conditions are marked by the deposition of sulfides, predominantly pyrrhotite.

Extensive oceanic hydrothermal alteration is recognized in the volcanic rocks of the Serra do Itaberaba Group (Pérez-Aguilar *et al.*, 2000), being the diagnostic metamorphic minerals anthophyllite, gedrite, cummingtonite and cordierite. The altered rocks lie in the vicinity of the iron formation and gold mineralization and are associated with margarite-corindon schists (marundites), resultant from advanced argillic alteration (Juliani, 1993).

Calc-silicate rocks, distributed around syn-volcanism intermediate rock intrusions, constitute less than 50 m-thick lenticular bodies composed of epidote-actinolite, phlogopite-actinolite-diopside and calcite-epidote-actinolite schists alternating with epidote-rich and tremolite-actinolite- and diopside-rich bands. Subordinately phlogopite, tourmaline, carbonates and opaque minerals occur. The lenses that lie, for example, at the base of the iron formation and grade laterally to metapelites, suggest the origin of calc-silicate rocks from exhalative volcanic activities.

Banded iron formation occurs as intercalations in the terrigenous and volcanic metasediments deposited on the metavolcanic rocks. They were deposited in zones farther from the coast and more internal to the basin. The compositional variations, essentially chemical and pelagic, characterize this unit as of the Algoma type, according to Gross (1965, 1980).

The subduction of the oceanic crust to the east forced the development of a back-arc basin. The basin was filled with sediments coming from both the island arcs and the foreland. The waters became shallower with the closing of the back-arc basin and the intense exhalative volcanic activity led to the deposition of the Nhanguçu Formation. It is essentially represented by iron-manganesiferous schists with small lenses of carbonate rocks and calc-pelites, covered by andalusite-rich schists.

The Pirucaia Formation is composed of quartzites and rhythmic quartz schists, deposited by turbidity currents in a coastal environment.

Partly deformed porphyritic granite and granodiorite bodies, such as Pau Pedra and Serra da Pedra Branca (Juliani, 1993), intruded the Serra do Itaberaba Group in the Neoproterozoic. These may be an extension of the syn- to late-orogenic, calc-alkaline, 625 Ma-old Cantareira granitoid magmatism described in Janasi & Ulbrich (1991).

The Rio Jaguari and Jundiuvira shear zones and associated faults affected the whole area, where the Neoproterozoic São Roque Group also crops out.

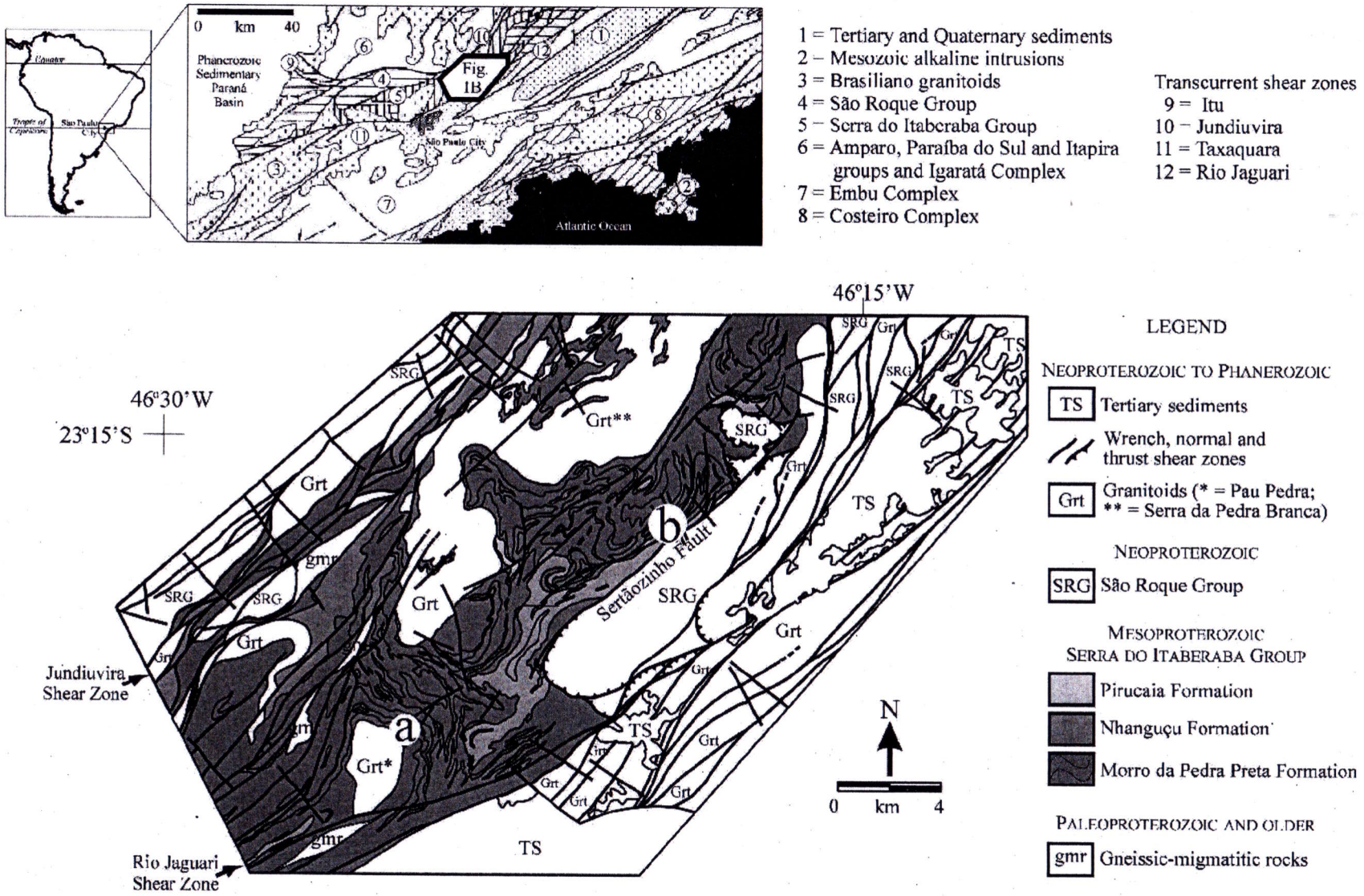

Figure 1a – Geological map of southeastern São Paulo State (modified after Almeida *et al.*, 1981)
Figure 1b – Simplified map of Serra do Itaberaba and São Roque groups (modified after Juliani, 1993). a = Tapera Grande (Fig. 2); b= Quartzito (Fig. 3)

MINERALIZATIONS IN THE MORRO DA PEDRA PRETA FORMATION

Two areas were selected for the present study: Tapera Grande (NE of Pau Pedra granitoid - [a] in Fig. 1b) and Quartzito (W of Sertãozinho Fault - [b] in Fig. 1b).

Mapping, semi-detail and detail prospecting in the Serra do Itaberaba Group allowed to individualize several bodies of volcaniclastic rocks with traces of gold and the preliminary outline of auriferous colluvia (IPT, 1985; Beljavskis, 1988; Juliani, 1993), in particular in Tapera Grande, including the Ribeirão das Lavras old mining activities (Fig. 2). An exploration program was set forth to better understand the geometry, position of the mineralized bodies and the preliminary quantification of the auriferous mineralizations. Soil geochemistry detected W and low Cu, Pb and Zn contents associated with gold.

In Tapera Grande, samples from B and C soil profiles, taken from the walls and the floor of old mining activities, yielded 0.5-13.0 g/t Au and 0.64-7.8 g/t Ag (IPT, 1985; Beljavskis, 1988; Beljavskis & Born, 1989; Beljavskis & Born, 1992). Eleven drill holes sampled varied banded schists, iron formations, metatuffs, graphite schists, volcaniclastic rocks, calc-silicate rocks and metabasites of the Morro da Pedra Preta Formation. The mineralized zone is located in the interface between basic volcanic/volcaniclastic flows and metapelites and calc-silicate rocks (Fig. 2). It extends for more than 5 km and is mainly associated with basic and intermediate metatuffs, which are in general silicified, carbonatized and potassified, and metandesite/metadacite intrusions. It is also recognized in sulfidized graphitic metapelites. The sulfides associated with gold are essentially pyrrhotite and subordinate pyrite and chalcopyrite, and occur either disseminated or remobilized forming blebs and/or films in microfractures, aggregates among the volcanic fragments, and thin laminae in metapelites. Scheelite occurs as trace mineral, only in the intermediate rocks.

In Quartzito (Fig. 3), fourteen rotary drill holes were carried out by IPT, ten of which in the Q-10 target (IPT, 1993). The mineralized body Q-10, striking E-W to N50E and dipping 27°SE, corresponds to a strongly sheared iron formation, showing remobilization and recrystallization of quartz and hematite. It is predominantly constituted by a ferruginous metachert, positioned between metatuffs (chlorite-quartz schists) and calc-silicate rocks. The ferruginous metachert stretches out for 1500 m, with thicknesses varying from 1.5 to 35 m northwards. Marundites, metapelites, calc-silicate rocks, basic metatuffs and metabasites of the Morro da Pedra Preta Formation are also recognized in the area. The whole sequence is crosscut by the Sertãozinho Fault and associated fracturing. Structures with direction between N30-60E predominate (IPT, 1993).

Drill holes FQ-112 and FQ-114 are of special interest once they sampled the whole Morro da Pedra Preta Formation lithologic sequence. FQ-112 crosscuts rocks of intermediate composition that present an ample textural variety, including portions with volcaniclastic rocks and metatuffs. Sulfides are found both disseminated and filling microfractures. Quartz veins, notably those associated with breccia zones, bear sulfides and variable quantities of tourmaline. Scheelite and molybdenite, besides gold, were also detected in FQ-112 core samples.

SULFIDATION STAGES

In this work, the term sulfidation refers to the formation of sulfide minerals. Beljavskis *et al.* (1999a, 1999b) defined four sulfidation stages that affected the Tapera Grande and Quartzito areas, based on conventional ore petrography and mineral analyses and imagery by SEM-EDS:

Stage I – The predominant sulfide is pyrrhotite, with very subordinate pyrite in graphitic schists, forming very foliated films and thin lenses parallel with graphitic laminae that alternate with sericite- and/or biotite-rich thin laminae, with or without subordinate quartz. The closer to the basic flows the higher is the sulfide content, where up to 2 cm-thick sulfide-rich laminae and bands occur. The sulfide laminae are intrafolial folded by the first deformational event and the disseminated sulfides were engulfed by the first porphyroblasts along bedding tracks, indicating a pre-metamorphic origin. The original sulfide, due to reducing depositional conditions, must have been hexagonal pyrrhotite, precipitated under low temperatures (Vaughan & Craig, 1978; Craig & Scott, 1982); it further recrystallized as monoclinic pyrrhotite during the medium-grade metamorphism. The texture shown in Figure 4a is explained by R.A. Ixer (pers. comm.) as pyrrhotite deposited together with the host

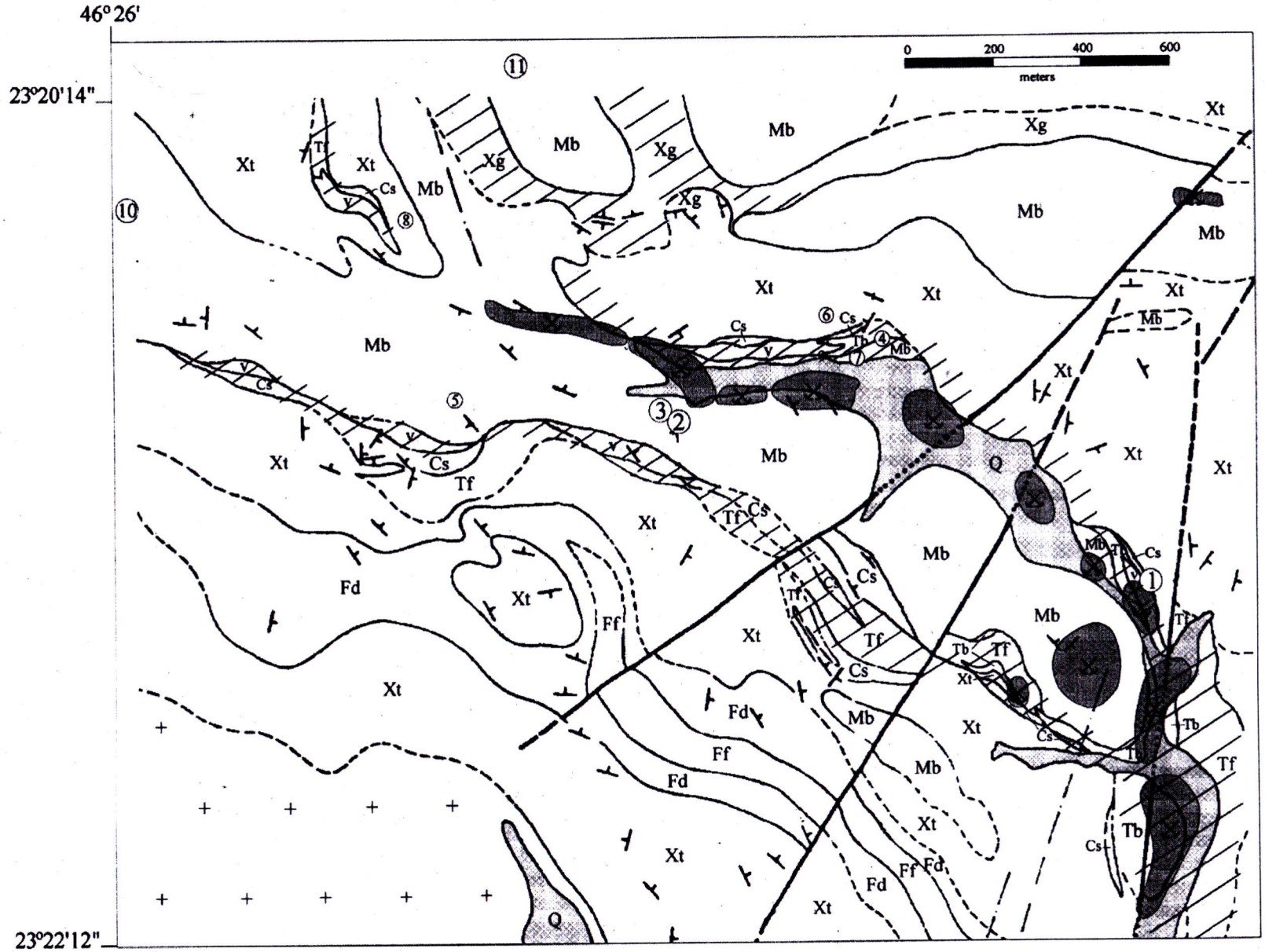

Figure 2 – Simplified geological map of Tapera Grande (area a in Fig. 1). Mineralized zones (hatched), old mining activities (dark gray) and Quaternary alluvial deposites (light gray) lie along Ribeirão das Lavras (not represented). Numbered circles are drill holes labelled SRT in the text.

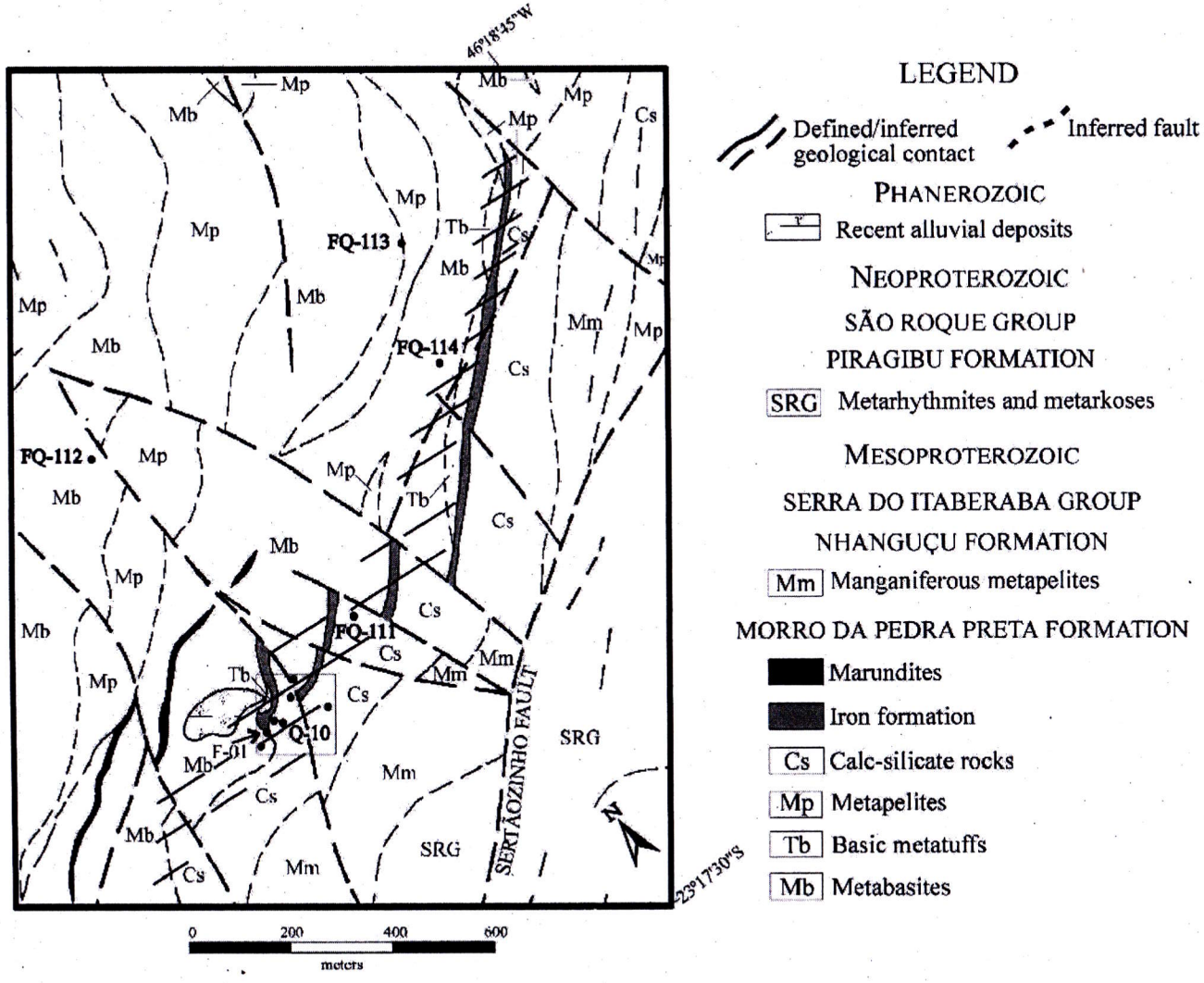

Figure 3 – Simplified geological map of Quartzito (area b in Fig. 1), modified after IPT (1993). Dark circles represent drill holes. Hatching represents mineralized zones.

graphitic sediment, which was later altered to tabular intergrowths/overgrowths of euhedral pyrite and marcasite. Pyrite occurs associated with pyrrhotite in small amounts, indicating that pyrrhotite did not undergo significant alteration and recrystallization after the metamorphic peak, probably because the graphite content of the rock prevented the oxidation state to change, once pyrite is the main phase that incorporates S freed from pyrrhotite under lower temperatures (Craig & Vokes, 1993). The sulfide chemical recrystallization control in the graphitic schists is evidenced by pyrite enrichment. Pyrite becomes the predominant sulfide close and at the contact of metasediments and overlying basic rocks, where graphite content was lower and circulation of metamorphic fluids was more effective along the discontinuities between the layers.

SEM-EDS analyses in pyrrhotite revealed Fe contents averaging 61.08 wt%, which corresponds to temperatures of the order of 300-400°C at solvus conditions (Craig & Vokes, 1993), indicating that pyrrhotite still registers temperatures of the prograde metamorphism that reached the amphibolite facies. It is difficult to establish whether Stage I pyrrhotite was a primary phase or originated by desulfidation of syn-sedimentary pyrite during prograde metamorphism (Ferry, 1981); yet, it is remarkable that it registers metamorphic episodes. For this reason, it is referred in the text as "syn-sedimentary pyrrhotite".

Disseminated submicron-sized gold grains (*ca.* 1 mm), as well as zircon and monazite, were detected by SEM-EDS in graphite schists and correlated tourmalinite (Fig. 4b).

Stage II - Beljavskis *et al.* (1999b) explain that this stage differs from Stage I by higher base metal (Cu) contents. Stage II sulfides are disseminated, but sometimes constitute stringers in the basic volcaniclastic rocks deposited on the basalt flows and metandesites/metadacites. In the graphitic schists deformed and metamorphosed thin veinlets occur locally, truncating Stage I laminae.

In the hydrothermalized and gold-mineralized intermediate volcaniclastic rocks, pyrite predominates, associated with pyrrhotite and subordinate chalcopyrite. The sulfidation is related to quartz veinlets and associated carbonates and biotite, or to tourmaline-bearing metachert intercalated in the volcaniclastic rocks. Here, sulfide transformation was more effective, such as pyrrhotite substitution for pyrite, stretching, metamorphic agglutination and even sulfide recrystallization along later metamorphic foliations.

Stage II sulfides in Quartzito are associated with deformed quartz veins crosscutting metatuffs of the Morro da Pedra Preta Formation. These are pyrites of "porous" aspect, as shown in Figures 4f and 4g.

Stage III – This stage was responsible for the generation of veinlets that are partially discordant in relation to the S_2 foliation. They are tourmaline-rich and sometimes appear as conspicuous quartz veins, indicating that hydrothermalism took place at late stages of the second metamorphic event. The veins mainly crosscut metatuffs, metabasites and metasediments situated close to granitic intrusions in Tapera Grande (Fig. 1b) and are associated with shear, thrust and transcurrent fault zones in Quartzito.

In Quartzito, chalcopyrite appears either bordering (Fig. 4f) or filling cavities (Fig. 4g) of Stage II "porous" pyrite grains, or isolated or filling fractures of the host rock.

Millimeter-sized gold grains are disseminated in vein quartz and are associated with low-temperature Cu minerals (Fig. 4h), such as chalcocite (Fig. 4j) and covellite, supergene alteration minerals after chalcopyrite. Analyses by SEM-EDS indicate compositions of 95% Au and 5% Ag for the gold grains.

Stage IV – The last sulfidation stage is mainly associated with hydrothermal veins found in shear zones, bearing pyrite, chalcopyrite, galena and molybdenite. The veins show sericitic alteration, are fluorite- and tourmaline-rich, and are identical to late veins that crosscut granite bodies intrusive in the Serra do Itaberaba Group (Juliani, 1993), thus being interpreted as late hydrothermal fluids of magma crystallization. Less deformed or undeformed late quartz veins also occur.

In Tapera Grande, Stage IV sulfides are found in metavolcaniclastic rocks, not only filling microfractures in Stage II pyrite crystals (Figs. 4d and 4e), but also along the edges of the predominant minerals.

In Quartzite, the veins are closely related to shear zones and Stage IV sulfides are associated with late fractures in Stage III sulfide-bearing quartz veins crosscutting metavolcaniclastic rocks. Chalcopyrite and pyrite are partially replaced by Zn-Cd sulfides (Fig. 4i; Garda *et al.*, 1999). Molybdenite, native silver, electrum and galena were also identified, as well as Bi telurides, REE phosphates and scheelite.

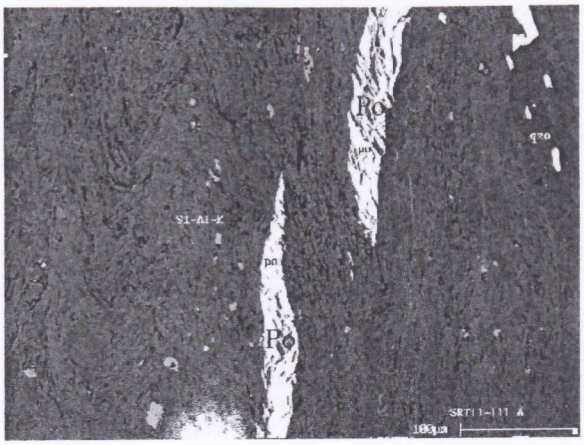

SRT11-111 A 4a 100µm

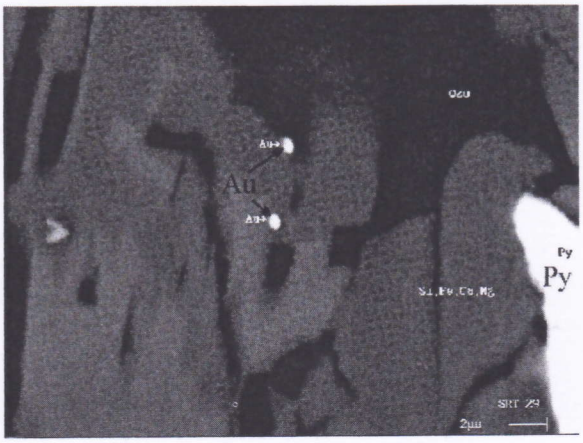

SRT 29 4b 2µm

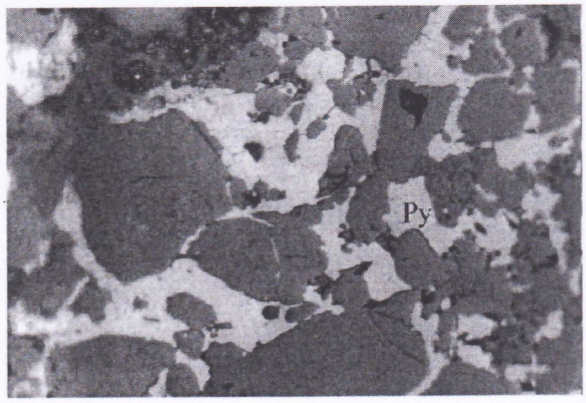

SRT3 (54.70-54.80m) 4c 0.34 mm

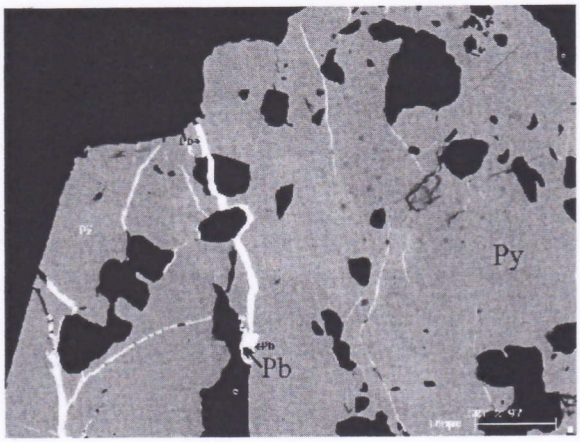

SRT2-97 4d 100µm

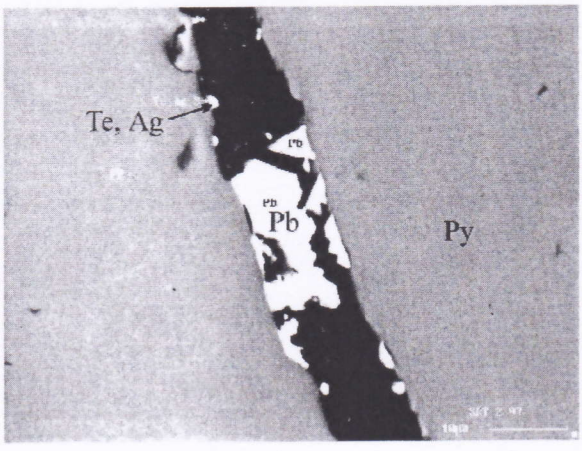

SRT2-97 4e 10µm

Po = pyrrhotite
Py, FeS = pyrite
Cpy = chalcopyrite
Cs = chalcosite
Cv = covellite
Pb = galena
Zn, Cd S = Zn-Cd sulfide
Ag = native silver
Te = telluride

Figure 4 – Scanning electron microscope images (a, b, d, e, h and i) and reflected light photomicrographs (c, f, g and j) of samples analysed for S stable isotopes. See text for description.

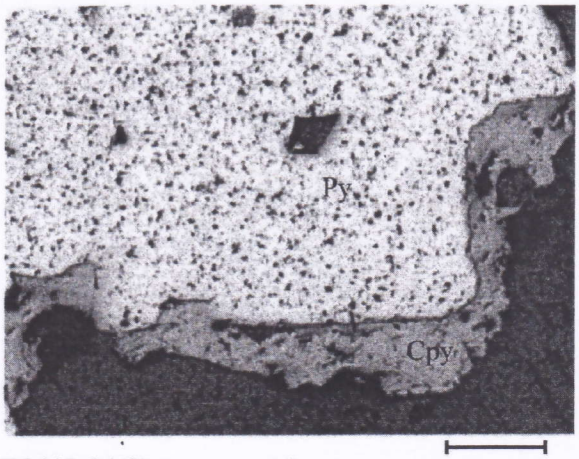

FQ112-34(2) 4f 1 mm

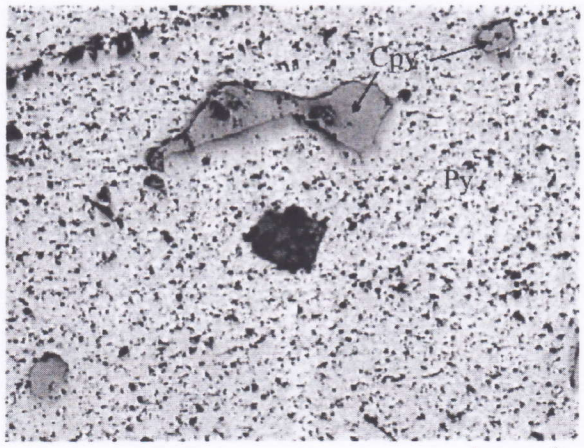

FQ112-34(2) 4g 1 mm

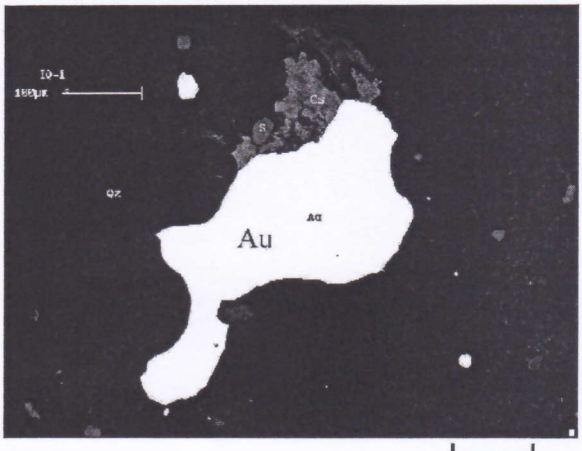

IQ-01 4h 100µm

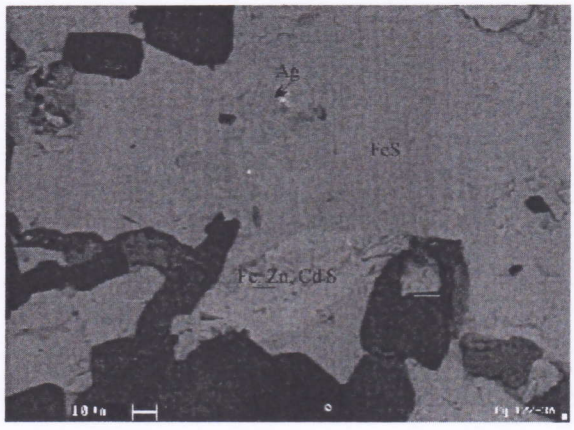

FQ112-3A 4i 10µm

Po = pyrrhotite
Py, FeS = pyrite
Cpy = chalcopyrite
Cs = chalcosite
Cv = covellite
Pb = galena
Zn, Cd S = Zn-Cd sulfide
Ag = native silver
Te = telluride

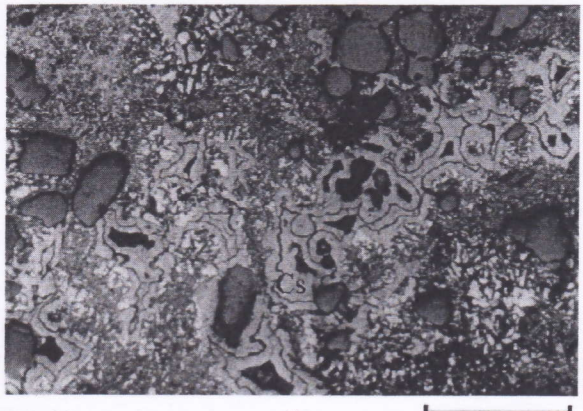

IQ-01 4j 0.34 mm

Figure 4 – (continuation)

STABLE ISOTOPES

Sulfur stable isotope studies were carried out at the Scottish Universities Environmental Research Centre (Glasgow, Scotland) by the conventional and laser methods of SO_2 extraction.

The **conventional method** of SO_2 extraction is based on the reaction between the sulfide and Cu_2O (Robinson & Kusakabe, 1975). Five to ten milligrams of sulfide are weighed together with 200-250 mg of reagent and manually mixed, using an agate mortar and pestle, and placed in a 3.2 cm-long glass tube in between some glass wool.

The reaction takes place at temperatures around 1075 °C for about 25 minutes in a furnace coupled on one of the ends of the extraction line. SO_2, H_2O, CO_2 and non-condensable gases are liberated from the reaction and SO_2 is isolated after the other gases are eliminated by means of traps and points along the line linked with the high vacuum system. SO_2 is collected in a sample bottle, which is then attached to the mass spectrometer (VG SIRA II®), yielding $\delta^{66}SO_2$ values.

The **laser method** enables *in situ* analyses with spatial resolution of ~ 100mm (Fallick *et al.*, 1992). The sample used is a polished block of approximately 4.0 cm x 2.4 cm x 0.7 cm. SO_2 and other gases are produced by the reaction between the sulfide and O_2 under high temperatures generated by the laser in a sample chamber kept under high vacuum. The SO_2 extraction is similar to what happens in the conventional method, once H_2O, CO_2, non-condensable gases, including O_2 in excess, are eliminated along the extraction line coupled on the sample chamber. SO_2 is sent directly to the mass spectrometer coupled on the end of the line.

All sulfur isotope results are expressed in conventional delta ($\delta^{34}S$) notation as per mil deviations relative to Cañon Diablo troilite.

Table 1 presents the results of sulfur isotope analyses corresponding to SO_2 extraction by the conventional method. Yield and $\delta^{34}S$ values are obtained by means of a computer program, given SO_2 values measured at the end of the extraction process and $\delta^{66}SO_2$ values obtained from the mass espectrometer.

Table 2 presents the results of sulfur isotope analyses corresponding to SO_2 extraction by the laser method. Kelley & Fallick (1990) point out that the isotopic composition measured is

Table 1 – Sulfur stable isotope analyses of sulfides of the Serra do Itaberaba Group (conventional method).

Sample	Sulfide	$\delta^{34}S$ (per mil)
STAGE I		
SRT-11-145	pyrrhotite	-7.30
STAGE II		
F-01 (1-A)	pyrite	7.58
FQ-112-46	pyrite	5.43
SRT-10-95	pyrite	5.20
FQ-112-43	pyrite	4.66

fractionated in relation to the real value; this fractionation depends on the laser-solid interaction. Fractionation factors, specific for certain sulfides, correct $\delta^{34}S$ values obtained from the computer program that gives $\delta^{34}S$ values for the gas.

Figure 5 presents a summary of the ranges of $\delta^{34}S$ values for each sulfidation stage and corresponding minerals. To Stage I pyrrhotites correspond negative $\delta^{34}S$ values, whereas decreasing, positive $\delta^{34}S$ values are related to Stages II to IV. It is worth mentioning that, for the supergene chalcocite (Fig. 4j), a value close to zero per mil was obtained.

DISCUSSION

One of the key roles of sulfur stable isotope geology is that it helps distinguish ore deposits related to igneous-hydrothermal activity from those of sedimentary origin. One of the facts that corroborates to the latter is that bacteria living in freshly deposited sediment reduce seawater sulfate and enrich the resulting H_2S in ^{32}S. Consequently, sulfur that has been subjected to bacterial reduction becomes enriched in ^{32}S compared to marine sulfate (Faure, 1986). Negative $\delta^{34}S$ values will result and good examples are given by Velasco *et al.* (1998), who obtained negative $\delta^{34}S$ values for diagenetic sulfide deposits of the Pyritic Iberic Belt, and Fallick *et al.* (2001), who suggest that more than 90% of the sulfides of the Zn-Pb deposits of Navan (Ireland) were derived through bacteriogenic reduction of Mississipian seawater sulfate, based on consistent negative $\delta^{34}S$ values averaging -13.6 ± 2 per mil.

Although isotopic composition of sulfur may be modified after deposition by thermal metamorphism (*e.g.* Faure, 1986; Wagner &

Table 2 – Sulfur stable isotope analyses of sulfides of the Serra do Itaberaba Group (laser method).

Sample	Point	Sulfide	$\delta^{34}S$ (per mil)
STAGE I			
SRT11-111	1	pyrrhotite	-8.70
SRT11-145	2	pyrrhotite	-7.88
SRT11-111	3	pyrrhotite	-7.49
SRT11-145	1	pyrrhotite	-7.36
SRT11-111	2	pyrrhotite	-6.71
SRT11-145	4	pyrrhotite	-6.60
SRT11-111	5	pyrrhotite	-6.15
SRT11-111	4	pyrrhotite	-5.47
STAGE II			
SRT1-2	3	pyrite	4.48
FQ112-34(2)	4	pyrite	4.70
SRT1-2	4	pyrite (+pyrrhotite)	4.71
SRT1-2	1	pyrite	4.87
SRT1-2	2	pyrrhotite	4.95
FQ112-34(2)	5	pyrite	5.19
FQ112-46(2)	4	pyrite	5.30
SRT3-99	1	pyrite	5.38
SRT3-99	2	pyrite	5.72
SRT2-97	4	pyrite	6.30
SRT2-97	2	pyrite	6.47
FQ112-34(2)	2	pyrite	6.62
SRT2-97	1	pyrite	7.05
SRT2-97	3	pyrite	7.36
STAGE III			
FQ112-34(2)	6	chalcopyrite	2.56
FQ112-34(2)	1	chalcopyrite	2.74
FQ112-34(2)	7	chalcopyrite	2.85
FQ112-3A	1	pyrite	2.90
FQ112-46(2)	2	molybdenite	3.01
FQ112-3A	2	chalcopyrite	3.63
STAGE IV			
FQ112-3A	4	galena	1.03
FQ112-34(2)	3	chalcopyrite	2.25
FQ112-46(2)	1	molybdenite	2.34
IQ-01	1	pyrite	2.38
SUPERGENE SULFIDES			
IQ-01	2	pyrite+ chalcopyrite+ chalcosite	-0.04

Boyce, 2001), negative $\delta^{34}S$ values can still indicate original isotopic signatures, even after metamorphism and recrystallization (McKibben & Eldridge, 1989). For the Morro da Pedra Preta Formation, $\delta^{34}S$ values between –5.47 to –8.70 per mil correspond to Stage I "syn-sedimentary pyrrhotite" found in Tapera Grande graphite schists. The negative values alone would immediately suggest bacterial reduction of seawater sulfate; however, other geological factors must be taken into account, such as deposition environment and geotectonic regime. The graphitic sediments were deposited in the pelagic zone of the Morro da Pedra Preta back-arc basin, under the influence of oceanic hydrothermal systems powered by heat coming from andesite and dacite intrusions in the underlying basic flows (Juliani, 1993; Juliani & Beljavskis, 1995; Pérez-Aguilar, 2001). In such an environment, sulfide resulting from thermochemical reduction of seawater sulfate should yield positive $\delta^{34}S$ values similar to those obtained for Mesoproterozoic seawater sulfate (> 20 per mil; Lyons *et al.*, 2002). Fallick *et al.* (2001) and Blakeman *et al.* (2002) obtained positive $\delta^{34}S$ values reaching +15 per mil, considered representative of reduced sulfur transported to the site of deposition by hydrothermal fluids, and Maynard *et al.* (1997) obtained $\delta^{34}S$ values up to +6 per mil, corresponding to local reduction of seawater sulfate in the near subsurface around sea-floor vents and within the sulfide deposits themselves.

On the other hand, negative sulfur isotopic signatures can result from changes in the oxidation state or from seawater sulfate bacterial reduction. Higher oxidation state can be produced by liberation of H_2S and H_2 to the vapor phase by boiling (McKibben & Eldridge, 1989), but features linked to this process have not been recognized in the Serra do Itaberaba Group. Therefore, bacterial reduction of seawater sulfate must have been the main process responsible for the isotopic signature obtained for Stage I pyrrhotite. However, more significant negative values should be expected, implying that contributions from other sulfur sources - volcanogenic and from hydrothermal fluids exhaled from fumaroles nearby – occurred so that mixing of lighter and heavier sulfur isotopes yield intermediate $\delta^{34}S$ values, but the negative signature still prevailing (Fig. 6a).

Ample variations correspond to positive $\delta^{34}S$ values related to Stages II to IV (Fig. 5). Von

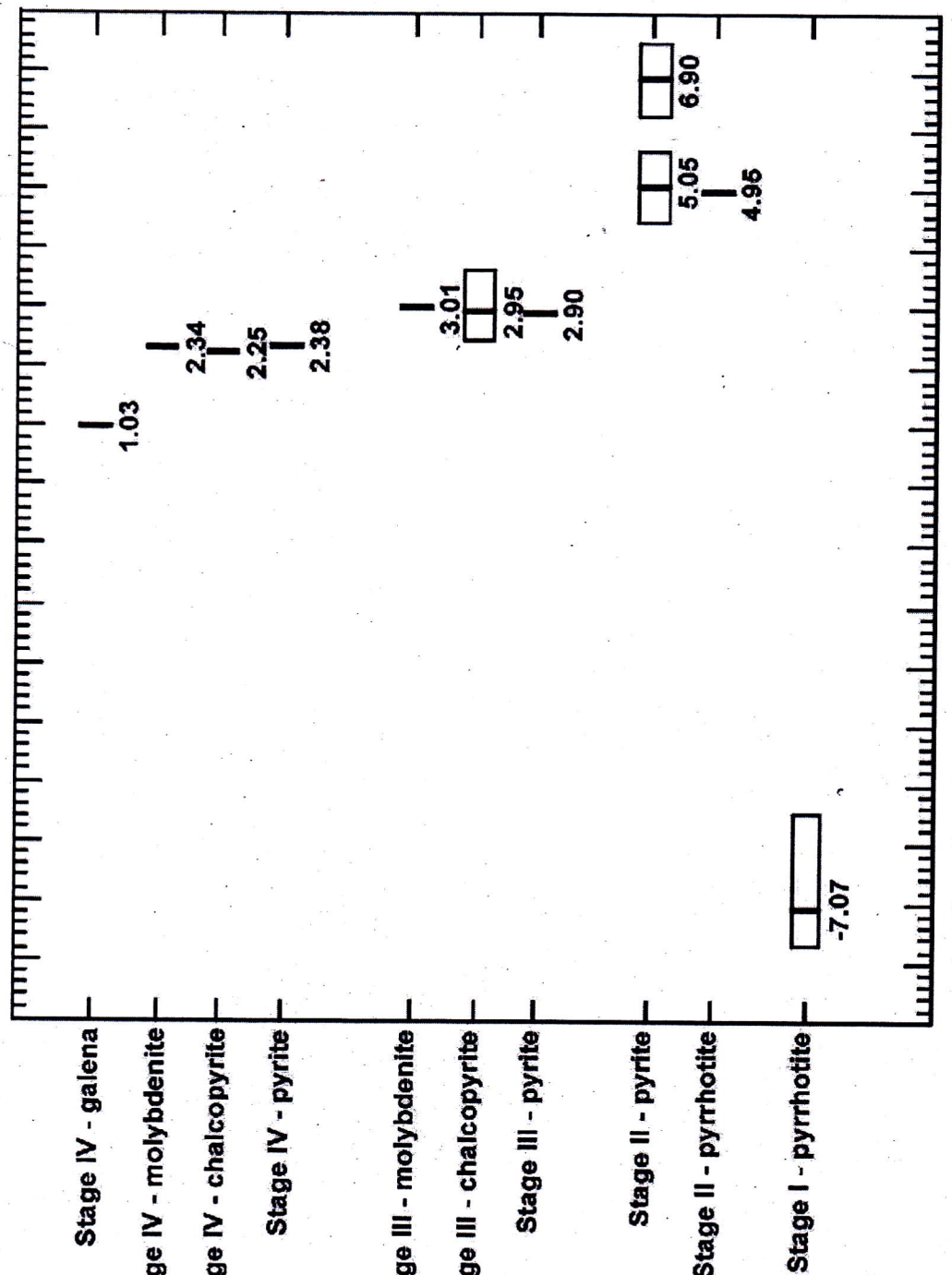

Figure 5 – Ranges of $\delta^{34}S$ values for each sulfidation stage and corresponding minerals. Mean $\delta^{34}S$ values for each range and single mineral values are indicated by bars.

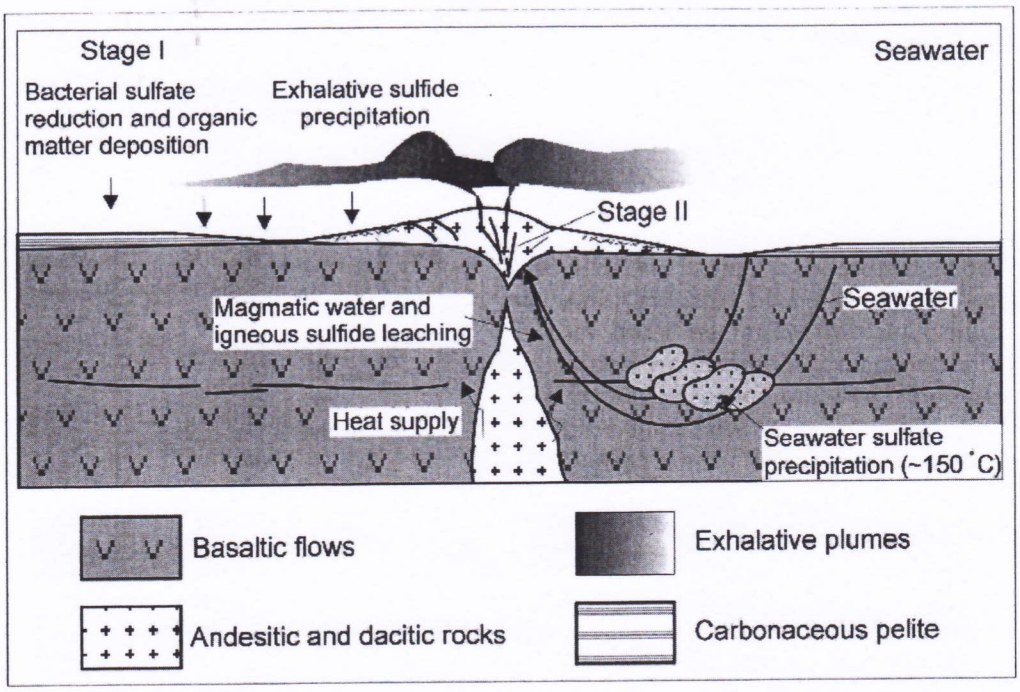

Figure 6a – Schematic diagram showing the formation of syn-depositional sulfides (Stages I e II). Together with organic matter deposition, there is mixing between hydrothermal sulfides and resulting from bacterial reduction of seawater sulfates.

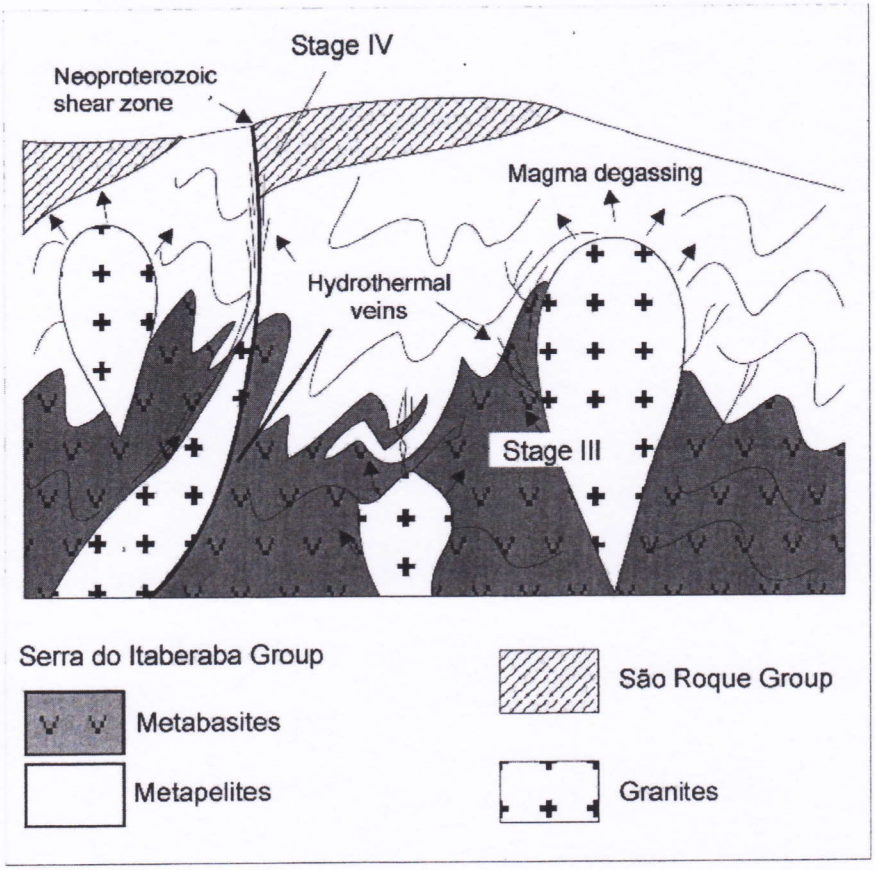

Figure 6b – Sktech indicating the geological environments of Stages III e IV sulfide formation during the Neoproterozoic.

Gehlen *et al.* (1983) verified that primary isotopic composition intervals can still be preserved by sulfides, even after metamorphic recrystallization in the amphibolite facies that partially re-equilibrates the isotopic composition of sulfur. This seems to be applicable to Tapera Grande Stage II sulfides. The range of +6.3 to +7.58 per mil (mean at +6.90 per mil) represents the highest $\delta^{34}S$ values obtained in this study, corresponding to gold-mineralized basic metatuffs of Tapera Grande. A second highest $\delta^{34}S$ interval of +4.48 to +5.72 per mil (mean at +5.05 per mil) corresponds to sulfides from volcaniclastic rocks and associated metatuffs overlain by metachert. These values fall in the intervals obtained for sulfides precipitated in MOR exhalative systems (Shanks, 2001), showing little participation of either fluids or sulfur originated from magma degassing.

In a back-arc environment, however, the contribution of a magmatic fluid with an igneous sulfur component is significant, resulting in $\delta^{34}S$ values close to zero per mil. This hypothesis should be applicable to Tapera Grande, as there is a close relationship between the andesite and dacite intrusions in the basic rock pile and the hydrothermal systems responsible for gold mineralization and sulfide deposition (Juliani, 1993; Juliani & Beljavskis, 1995).

The isotopic signature of Stage II sulfides can be explained by the circulation through the volcanic pile of seawater convection cells that, with increasing depth, are gradually heated; at temperatures around 150°C, sulfates (mainly anhydrite) precipitate in fissures of the volcanic rocks, causing the fluid to "partially lose" its heavy sulfur content. Closer to igneous intrusions, higher temperatures favor leaching and transport of metals and sulfur, derived from igneous sulfides present in the volcanic pile, which are then deposited below feeder zones and discharge vents (Alt, 1994; Shanks, 2001). Sulfides deposited by very hot hydrothermal fluids (350 to 400°C), either in ocean floor sulfur-mud or disseminated in the country rocks, especially below feeder zones, result in $\delta^{34}S$ signatures similar to those found in Tapera Grande. In these systems, the final isotopic signatures result from a complex mixture of sulfur from hydrothermal fluids (that may bear a quite strong igneous sulfur signature) and from sulfide originated from thermochemical reduction of small amounts of sulfates precipitated in fissures (Fig. 6a).

Stage III sulfides are predominantly represented by chalcopyrite (Table 2); a Stage III pyrite from one of the samples was also analysed and the values for both sulfides do not show significant $d^{34}S$ fractionation. Stage III $d^{34}S$ values are even lower than those for Stage II and vary between +2.56 and +3.63 per mil.

The emplacement of granite bodies in the Serra do Itaberaba Group (Fig. 1b) took place at the end of the São Roque metamorphic event that re-metamorphosed the Serra do Itaberaba Group. Quartz veins originated from late hydrothermal alteration are typically enriched in tourmaline in the salbands, and crosscut both the granites and the metavolcanic-sedimentary sequence. The crystallization of tourmaline along S_3 and S_4 foliations is also common, suggesting that magmatic fluids contributed to the final Neoproterozoic metamorphic fluids.

Thus, the $\delta^{34}S$ values obtained for Stage III can be attributed to mixture of sulfur from the volcanic-sedimentary sequence, leached by pervasive to fissure percolation of fluids derived from I-type granites, with the igneous sulfur itself ($\delta^{34}S$ values varying from -3.0 per mil to +3.0 per mil; *e.g.* Lowry *et al.*, 1997). Sulfides then precipitated in physical discontinuities, as late metamorphic foliations, shear zones, faults and fractures (Fig. 6b).

When Ohmoto's & Rye's (1979) geothermometers are applied to sulfide pairs of Stages II (pyrite-pyrrhotite) and III (pyrite-chalcopyrite), the resulting temperatures do not correspond to those obtained by other methods (*e.g.* microthermometry - Garda *et al.*, 2002), showing that the mineral phases are in disequilibrium, markedly in Quartzito. Isotopic disequilibrium is not an uncommon feature, as illustrated by Bluth & Ohmoto (1988) for hydrothermal vents along the East Pacific Rise.

In Quartzito, the disequilibrium may have been caused by remobilization processes assisted by fluids percolating the Sertãozinho shear zone and associated faults (Fig. 2). The Stage IV assemblage, composed of Zn-Cd sulfides replacing chalcopyrite and pyrite (Fig. 4I), molybdenite, native silver, electrum, galena, Bi telurides and REE phosphates, must be related to these fluids. $\delta^{34}S$ values for Stage IV sulfides fall in the interval of +1.03 to +2.38 per mil, being a little lower than those obtained for Stage III sulfides. This indicates that the channeling of granite-derived fluids in shear zones results in a less efficient mixture with sulfur derived from the volcanic-sedimentary

sequence and therefore these values are closer to those expected for sulfur derived from igneous sources, possibly with the increase of the oxidation state caused by mixture with meteoric water.

CONCLUDING REMARKS

Sulfur isotopic data helped constrain both syngenetic and epigenetic types of gold mineralization for Tapera Grande and Quartzito. Negative $\delta^{34}S$ values correspond to Stage I, "syn-sedimentary pyrrhotites" from Tapera Grande graphite schists. Neither metamorphism nor low-temperature alteration affected dramatically the primary sulfur isotopic composition. The detection of submicron-sized gold by SEM corroborates to the sulfur stable isotope data, that is, sulfides and associated gold of syngenetic origin.

Positive $\delta^{34}S$ values for Tapera Grande and Quartzito correspond to the epigenetic mineralization in the Serra do Itaberaba Group. Higher $\delta^{34}S$ values found for Stage II signal the role of hydrothermal fluids that result from seawater circulation in convection cells, powered by heat coming from the intrusion of andesitic and dacitic magmas, under a back-arc regime. Lower $\delta^{34}S$ values, relatively to the Mesoproterozoic seawater sulfate, result from "partial loss" of heavy sulfur due to precipitation at depth of sulfate present in the hydrothermal fluid; close to the hot andesite and dacite bodies, the circulating fluid is able to leach both sulfur from igneous sulfides in the volcanic pile and sulfur from the magma of intermediate composition. The sulfides deposited in the feeder zones, in the overlying volcanic and volcaniclastic rocks and sulfur-muds yield $\delta^{34}S$ signatures that are representative of mixing of heavy sulfur contents in the hydrothermal fluid, sulfur from the volcanic pile and magmatic sulfur (Fig. 6a). These data are consonant with Juliani's (1993) evolution model for the Serra do Itaberaba Group.

Stage III fluids result from mixing of hydrothermal fluids with fluids derived from degassing of I-type magmas in the Neoproterozoic (Fig. 6b). Pyrite and chalcopyrite are conspicuous opaque minerals associated with the epigenetic mineralization.

The Stage IV assemblage composed of Zn-Cd sulfides replacing chalcopyrite and pyrite, molybdenite, native silver, electrum, galena, Bi telurides and REE phosphates are related to late fluids derived from granite genesis that percolated shear zones and associated faults, possibly affected by meteoric water (Fig. 6b).

The absence of gold as inclusions in chalcopyrites and pyrites associated with quartz veins is remarkable. Millimeter-sized gold grains (Fig. 4h) were found associated with chalcocite and covellite formed after chalcopyrite, which corroborates with the suggestion of meteoric water influencing late sulfidation stages.

ACKNOWLEDGEMENTS

The authors wish to thank Prof. Anthony E. Fallick for the facilities at the Scottish Universities Environmental Research Centre (Glasgow, Scotland) and FAPESP – São Paulo State sponsoring agency, for financial support for both stable isotope analyses (Proc. FAPESP 99/05792-3) and scanning electron microscope studies at Escola Politécnica - USP (Proc. FAPESP 95/3665-3) and Instituto de Geociências - UNICAMP (Proc. FAPESP 98/05526-9).

REFERENCES

ALMEIDA, F.F.M. de; HASUI, Y.; PONÇANO, W.L.; DANTAS, A.S.L.; CARNEIRO, C.D.R.; MELO, M.S. de; BISTRICHI, C.A. (1981) Mapa geológico do Estado de São Paulo, escala 1:500.000 - Nota explicativa. Instituto de Pesquisas Tecnológicas do Estado de São Paulo, 126p.

ALT, J.C. (1994) A sulfur isotopic profile through the Troodos ophiolite, Cyprus: primary composition and the effects of seawater hydrothermal alteration. Geochim. Cosmochim. Acta, **58**:1825-1840.

BELJAVSKIS, P. (1988) Prospecção geoquímica experimental na ocorrência de ouro Tapera Grande - Guarulhos - SP. M.Sc. Dissertation. Escola Politécnica, Universidade de São Paulo, 161p.

BELJAVSKIS, P. & BORN, H. (1989) Estudos litogeoquímicos na ocorrência de ouro Tapera Grande - Guarulhos - SP. *In:* Simp. Geol. Sudeste, 1, Rio de Janeiro. SBG, Boletim de Resumos, p.87-88.

BELJAVSKIS, P. & BORN, H. (1992) Prospecção geoquímica experimental na ocorrência de ouro de Tapera Grande. Boletim Técnico da Escola Politécnica da USP, **2**:18p.

BELJAVSKIS, P.; GARDA, G.M.; JULIANI, C. (1993) Características das mineralizações auríferas no Grupo Serra do Itaberaba, Guarulhos, SP. Rev. Instituto Geológico, **14**(1):21-29.

BELJAVSKIS, P.; GARDA, G.M.; SAYEG, I.J. (1999a) Application of SEM in the study of gold mineralizations in the Morro da Pedra Preta Formation, Grupo Serra do Itaberaba – São Paulo, Brazil. Acta Microscópica, 8(Supplement A):125-126.

BELJAVSKIS, P.; JULIANI, C.; GARDA, G.M.; XAVIER, R.P.; BETTENCOURT, J.S. (1999b) Overview of the gold mineralization in the metavolcanic-sedimentary sequence of the Serra do Itaberaba Group – São Paulo – Brazil. *In:* C.J. STANLEY (Coord. 1999) Mineral Deposits: Processes to Processing. Balkema, 1:151-153.

BELJAVSKIS, P.; XAVIER, R.P.; GARDA, G.M. (2000) Fluid inclusion studies of Au-bearing quartz veins – Serra do Itaberaba Group, São Paulo, Brazil. *In:* International Geol. Congr., 31, Rio de Janeiro. Abstracts Volume (CD-ROM).

BLAKEMAN, R.J.; ASHTON, J.H.; BOYCE, A.J.; FALLICK, A.E.; RUSSELL, M.J. (2002) Timing of interplay between hydrothermal and surface fluids in the Navan Zn + Pb orebody, Ireland: evidence from metal distribution trends, mineral textures, and $\delta^{34}S$ analyses. Econ. Geol., 97:73-91.

BLUTH, G.J. & OHMOTO, H. (1988) Sulfide-sulfate chimneys on the East Pacific Rise, 11∞ and 13∞N latitudes. Part II: sulfur isotopes. Can. Mineral., **26**:505-515.

CRAIG, J.R. & SCOTT, S.D. (1982) Sulfide phase equilibria. *In*: P.H. RIBBE (Ed.) Sulfide Mineralogy. Reviews in Mineralogy, 1: **CS1-CS110.**

CRAIG, J.R. & VOKES, F.M. (1993) The metamorphism of pyrite and pyritic ores: an overview. Mineral. Mag., **57**:3-18.

FALLICK, A.E.; MCCONVILLE, P.; BOYCE, A.J.; BURGESS, R.; KELLEY, S.P. (1992) Laser microprobe stable isotope measurements on geological materials: some experimental considerations (with special reference to $\delta^{34}S$ in sulfides). Chem. Geol., **101**:53-61.

FALLICK, A.E.; ASHTON, J.H.; BOYCE, A.J.; ELLAM, R.M.; RUSSELL, M.J. (2001) Bacteria were responsible for the magnitude of the world-class hydrothermal base metal sulfide orebody at Navan, Ireland. Econ. Geol., **96**:885-890.

FAURE, G. (1986) Principles of isotope geology. 2nd Ed. John Wiley & Sons, 589p.

FERRY, J.M. (1981) Petrology of graphitic sulfide-rich schists from south-central Maine: an example of desulfidation during prograde regional metamorphism. Am. Mineral., **66**:908-930.

GARDA, G.M.; BELJAVSKIS, P.; SAYEG, I.J. (1999) Gold mineralization in the Quartzito area, the Serra do Itaberaba Group – São Paulo, Brazil. Acta Microscópica, **8**(Supplement A):127-128.

GARDA, G.M.; BELJAVSKIS, P.; SILVA, D. (2002) Fluid inclusions in quartz from veins and metachert of the Au-bearing Serra do Itaberaba Group, São Paulo, Brazil. *In:* General Meeting of the International Mineralogical Association, 18th, Edinburgh (Scotland). I

GROSS, G.A. (1965) Geology of iron deposits in Canada. 1. General geology and evaluation of iron deposits. Geological Survey of Canada, Economic Geology Report 22, 181p.

GROSS, G.A. (1980) A classification of iron formations based on depositional environments. Can. Mineral. **18**(2):215-222.

HACKSPACHER, P.; DANTAL, E.L; GODOY, A.M.; OLIVEIRA, M.A.F. DE; FETTER, A.; VAN SCHUMUS, W.R. (1999) Considerations about the evolution of the Ribeira Belt in the São Paulo State - Brazil, from U/Pb geochronology in metavolcanic rocks of the São Roque Group. *In:* South American Symp. Isot. Geol., 2, Vila Carlos Paz, Argentina. Anais, p.192-195.

INSTITUTO DE PESQUISAS TECNOLÓGICAS DO ESTADO DE SÃO PAULO (1981) Avaliação preliminar das potencialidades das ocorrências minerais do Estado de São Paulo. São Paulo, IPT, 2v. (Report 15.849).

INSTITUTO DE PESQUISAS TECNOLÓGICAS DO ESTADO DE SÃO PAULO (1982) Ouro no Estado de São Paulo - Avaliação das ocorrências selecionadas. São Paulo, IPT, 2v. (Report 16.680)

INSTITUTO DE PESQUISAS TECNOLÓGICAS DO ESTADO DE SÃO PAULO (1984) Projeto Ouro Tapera Grande - Pesquisa de detalhe. São Paulo, IPT, 3v. (Report 20.719)

INSTITUTO DE PESQUISAS TECNOLÓGICAS DO ESTADO DE SÃO PAULO (1985) Projeto prospecção para metais base na seqüência vulcano-sedimentar de Itaberaba, SP. São Paulo, IPT. (Report 22.434)

INSTITUTO DE PESQUISAS TECNOLÓGICAS DO ESTADO DE SÃO PAULO (1986) Estudos petrológicos da seqüência vulcano-sedimentar de Itaberaba - SP. São Paulo, IPT, 2v. (Report 24.510)

INSTITUTO DE PESQUISAS TECNOLÓGICAS DO ESTADO DE SÃO PAULO (1987) Prospecção mineral na região da Serra de Itaberaba - SP. Detalhe em alvos selecionados. São Paulo, IPT, 2v. (Report 25.298)

INSTITUTO DE PESQUISAS TECNOLÓGICAS DO ESTADO DE SÃO PAULO (1988) Prospecção geoquímica experimental na área de Tapera Grande. São Paulo, IPT/PRÓ-MINÉRIO, 282 p. (Report 26.005)

INSTITUTO DE PESQUISAS TECNOLÓGICAS DO ESTADO DE SÃO PAULO (1993) Bauxita e ouro. Relatório final de pesquisa. 32p. Anexos. (DNPM 820.183/82).

JANASI, V. & ULBRICH, H.H.G.J. (1991) Late Proterozoic granitoid magmatism in the state of São Paulo, southeastern Brazil. Precambrian Res., **51**:351-374.

JULIANI, C. (1993) Geologia, petrogênese e aspectos metalogenéticos dos grupos Serra do Itaberaba e São Roque na região das Serras do Itaberaba e da Pedra Branca, NE da cidade de São Paulo, SP. Tese de doutoramento. Instituto de Geociências, Universidade de São Paulo, 684p.

JULIANI, C. & BELJAVSKIS, P. (1983) Geologia e evolução geológico-estrutural preliminar do grupo São Roque na região da Serra do Itaberaba (SP). *In:* Simp. Reg. Geol., 4, São Paulo. SBG, Atas, p.113-126.

JULIANI, C. & BELJAVSKIS, P. (1995) Revisão da litoestratigrafia da Faixa São Roque/Serra do Itaberaba (SP). Rev. Instituto Geológico, **16**(1/2):33-58.

JULIANI, C.; BELJAVSKIS, P.; SCHORSCHER, J.H.D. (1986) Petrogênese do vulcanismo e aspectos metalogenéticos associados: Grupo Serra do Itaberaba na região do São Roque - SP. *In:* Congr. Bras. Geol., 34, Goiânia. SBG, Anais **2**:730-745.

JULIANI, C.; BELJAVSKIS, P.; OLIVEIRA-JULIANI, L.J.C.; GARDA, G.M. (1995) As mineralizações de ouro de Guarulhos e os métodos de sua lavra no período colonial. Geol. Ciência-Técnica, **13**:8-25.

JULIANI, C.; HACKSPACHER, P.; DANTAS, E.L.; FEITER, A.H. (2000) The Mesoproterozoic volcano-sedimentary Serra do Itaberaba Group of the central Ribeira Belt, São Paulo State, Brazil: implications for the age of the overlying São Roque Group. Rev. Bras. Geoc., **30**(1):82-86.

KELLEY, S.P. & FALLICK, A.E. (1990) High precision spatially resolved analysis of $\delta^{34}S$ in sulfides using a laser extraction technique. Geochim. Cosmochim. Acta, **54**:883-888.

LOWRY, D.; BOYCE, A.J.; FALLICK, A.E.; STEPHENS, W.E. (1997) Sources of sulphur, metals and fluids in granitoid-related mineralization in the Southern Uplands, Scotland. Trans. Instn. Min. Metall. (Sect. B: Appl. Earth Sci.), **106**:B157-B168.

LYONS, T.W.; GELLATLY, A.M.; FRANK, T.D.; KAH, L.C. (2002) Chemistry of the Mesoproterozoic ocean and links to biospheric oxygen levels. *In:* Astrobiology Science Conference, 2, Ames (California, USA). NASA Abstracts: http://www. astrobiology.com/ asc2002/abstract.html?ascid=135.

MAYNARD, J.; PRICHARD, H.M.; IXER, R.A.; LORD, R.A.; WRIGHT, I.P.; PILLINGER, C.T.; MCCONVILLE, P.; BOYCE, A.J.; FALLICK, A.E. (1997) Sulphur isotope study of Ni-Fe-Cu mineralization in the Shetland ophiolite. Trans. Instn. Min. Metall. (Sect. B: Appl. Earth Sci.), **106**:B215-B226.

McKIBBEN, M.A. & ELDRIDGE, C.S. (1990) Radical sulfur isotope zonation in pyrite accompanying boiling and epithermal gold deposition: a SHRIMP study of the Valles Caldera, New Mexico. Econ. Geol., **85**:1917-1925.

NORONHA, A.V. (1960) Guarulhos, cidade símbolo. História de Guarulhos. Schmidt, 113p.

OHMOTO, H. & RYE, R.O. (1979) Isotopes of sulfur and carbon. *In:* H.L. BARNES (Ed.) Geochemistry of hydrothermal ore deposits. John Wiley & Sons, p.509-567.

PÉREZ-AGUILAR, A. (2001) Petrologia e litogeoquímica de rochas de paleossistemas hidrotermais oceânicos mesoproterozóicos da seqüência metavulcanossedimentar do Grupo Serra do Itaberaba, SP. Tese de doutoramento. Instituto de Geociências, Universidade de São Paulo, 223p.

PÉREZ-AGUILAR, A.; JULIANI, C.; MARTIN, M.A.B. (2000) Mesoproterozoic paleo-hydrothermal system in the Morro da Pedra Preta Formation, Serra do Itaberaba Group, São Paulo State, Brazil. Rev. Bras. Geoc., **30**(3):409-412.

PIRES, F.A.; FERNANDES, A.J.; TEIXEIRA, A.L.; BOGGIANI, P.C.; MASSOLI, M.; PETRI, S. (1990) Mapa geológico da Folha Salto de Pirapora - SP (SF-23-Y-C-IV-2), na escala 1:50.000. *In:* Congr. Bras. Geol., 36, Natal. SBG, Boletim de Resumos, 352p.

ROBINSON, B.W. & KUSAKABE, M. (1975) Quantitative preparation of sulfur dioxide, for $^{34}S/^{32}S$ analyses, from sulfides by combustion with cuprous oxide. Anal. Chem., **47**(7):1179-1181.

SHANKS, W.C. (2001) Stable isotopes in seafloor hydrothermal systems: vent fluids, hydrothermal deposits, hydrothermal alteration, and microbial processes. Stable Isotope Geochemistry, **43**: 469-525.

VAUGHAN, D.J. & CRAIG, J.R. (1978) Mineral chemistry of metal sulfides. Cambridge University Press, 477 p.

VELASCO, F.; SÁNCHEZ-ESPAÑA, J.; BOYCE, A.J.; FALLICK, A.E.; SÁEZ, R.; ALMODÓVAR, G.R. (1998) A new sulfur isotopic study of some Iberian Pyrite Belt deposits: evidence of a textural control on sulfur isotope composition. Miner. Deposita, **34**:4-18.

VON GEHLEN, K.; NIELSEN, H.; CHUNNETT, I.; ROZENDAAL, A. (1983) Sulphur isotopes in metamorphosed Precambrian Fe-Pb-Zn-Cu sulphides and baryte at Aggeneys and Gamsberg, South Africa. Mineral. Mag., **47**(4):481-486.

WAGNER, T. & BOYCE, A.J. (2001) Sulphur isotope characteristics of recrystallization, remobilisation and reaction processes: a case study from the Ramsbeck Pb-Zn deposit, Germany. Miner. Deposita, **36**:670-679.